HHS Public Access

Author manuscript

J Mater Chem C Mater Opt Electron Devices. Author manuscript; available in PMC 2017 August 07.

Published in final edited form as:

J Mater Chem C Mater Opt Electron Devices. 2016 August 7; 4(29): 6967–6974. doi:10.1039/C6TC01932C.

Enhanced Fluorescence Properties of Carbon Dots in Polymer Films

Yamin Liu[a], **Ping Wang**[a], **K. A. Shiral Fernando**[b,*], **Gregory E. LeCroy**[a], **Halidan Maimaiti**[a], **Barbara A. Harruff-Miller**[b], **William K. Lewis**[c], **Christopher E. Bunker**[c,*], **Zhi-Ling Hou**[a], and **Ya-Ping Sun**[a,*]

[a]Department of Chemistry and Laboratory for Emerging Materials and Technology, Clemson University, Clemson, South Carolina 29634

[b]University of Dayton Research Institute, Sensors Technology Office, Dayton, Ohio 45469

[c]Air Force Research Laboratory, Propulsion Directorate, Wright-Patterson Air Force Base, Ohio 45433

Abstract

Carbon dots of small carbon nanoparticles surface-functionalized with 2,2′-(ethylenedioxy)bis(ethylamine) (EDA) were synthesized, and the as-synthesized sample was separated on an aqueous gel column to obtain fractions of the EDA-carbon dots with different fluorescence quantum yields. As already discussed in the literature, the variations in fluorescence performance among the fractions were attributed to the different levels and/or effectiveness of the surface functionalization-passivation in the carbon dots. These fractions, as well as carbon nanoparticles without any deliberate surface functionalization, were dispersed into poly(vinyl alcohol) (PVA) for composite films. In the PVA film matrix, the carbon dots and nanoparticles exhibited much enhanced fluorescence emissions in comparison with their corresponding aqueous solutions. The increased fluorescence quantum yields in the films were determined quantitatively by using a specifically designed and constructed film sample holder in the emission spectrometer. The observed fluorescence decays of the EDA-carbon dots in film and in solution were essentially the same, suggesting that the significant enhancement in fluorescence quantum yields from solution to film is static in nature. Mechanistic implications of the results, including a rationalization in terms of the compression effect on the surface passivation layer (similar to a soft corona) in carbon dots when embedded in the more restrictive film environment resulting in more favorable radiative recombinations of the carbon particle surface-trapped electrons and holes, and also potential technological applications of the brightly fluorescent composite films are highlighted and discussed.

Introduction

Optical properties of carbon nanomaterials have attracted much recent attention for their variety of potential technological applications, from optoelectronics, bioimaging and sensing, to photocatalysis for energy conversion. Most of these materials are fluorescent

* yaping@clemson.edu. KAShiral.Fernando@udri.udayton.edu. christopher.bunker@wpafb.af.mil.

over the visible spectrum, extending into the near-IR. More specifically, carbon "quantum" dots or carbon dots were found and developed as a new class of brightly fluorescent nanomaterials,[1,2] with their performance competitive to that of conventional semiconductor quantum dots (QDs) yet nontoxic and environmentally benign.[3–5] In fact, carbon dots have emerged to represent now a rapidly advancing and expanding research field, as reflected by the large number of recent publications in the literature, with extensive investigations looking into many aspects of carbon dots for both fundamental and technological purposes.[3–16]

Carbon dots are generally defined as small carbon nanoparticles with various surface passivation schemes, including especially the surface functionalization by organic and bio-molecular species (Figure 1).[1,6,14,17,18] While fluorescence emissions from "naked" carbon nanoparticles (without any deliberate surface functionalization) in aqueous or other suspensions have been observed and reported,[19–23] their intensities are low, with observed quantum yields generally on the order of 1–2% or less. Therefore, effective surface passivation in carbon dots is necessary for bright fluorescence emissions.[3,4,6,14] For example, Wang, *et al.* reported that for carbon dots with oligomeric poly(ethylene glycol) diamine (PEG_{1500N}) as the surface passivation agent, the as-synthesized sample exhibited fluorescence quantum yields around 20%, from which more fluorescent fractions corresponding to carbon dots of more effective surface functionalization and passivation could be isolated to achieve fluorescence quantum yields of more than 50%.[24] A number of other studies have also confirmed the critical role of surface passivation in determining the fluorescence brightness of the resulting carbon dots.[6,14,25] The mechanistic origin and implications of the surface passivation in carbon dots have also been explored.[6,12,26]

The widely cited mechanistic framework for carbon dots is such that the abundant surface defects in the small carbon nanoparticles must be playing an important role in the observed optical properties of carbon dots.[6,12,27–29] Upon photoexcitation there must be rapid charge separation in the carbon nanoparticles for the formation of electrons and holes, which are "trapped" at various surface sites, and radiative recombinations of the electrons and holes are responsible for the observed fluorescence emissions (Figure 1).[6,12,29] The more effective passivation in carbon dots might have stabilized the surface sites for the electrons and holes, enabling more efficient radiative recombinations to result in higher fluorescence quantum yields. Within such a mechanistic framework, the weak fluorescence emissions from naked carbon nanoparticles in aqueous or organic suspensions may be understood in term of surface passivation effect provided by the solvation.[12,23] Organic solvents are apparently more effective than water in this regard, and the presence of amino molecules in the carbon nanoparticle solutions enhances the passivation effect and therefore the fluorescence performance.[23] It may be expected in the same mechanistic framework that a compression of the surface passivation layer in carbon dots (Figure 1) could also enhance the passivation effect for brighter fluorescence emissions, as hinted by the results obtained from carbon dots in a more restrictive environment.[30] A more systematic examination on such an enhancement effect is in demand for significant mechanistic implications and also for the relevance to various technological applications of carbon dots, such as their uses in polymeric composites for fluorescence displays and/or the like.[31,32]

In the work reported here we dispersed carbon dots of different levels of surface functionalization (thus different fluorescence quantum yields), as well as carbon nanoparticles without any deliberate functionalization, into poly(vinyl alcohol) (PVA, a polymer widely employed in optical spectroscopic investigations) for composite films. In the PVA matrix, the carbon dots and nanoparticles exhibited much enhanced fluorescence emissions in comparison with their corresponding aqueous solutions. The increased fluorescence quantum yields in the films were determined quantitatively by using a specifically designed and constructed film sample holder in the emission spectrometer. Since the fluorescence decays of the carbon dots in film and in solution are essentially the same, the significant enhancement in fluorescence quantum yields from solution to film is attributed to static in nature, rationalized as a result of enhanced surface passivation for the carbon dots in a more confined environment in the PVA matrix. The mechanistic and technological implications of the results are discussed.

Experimental Section

Materials

Carbon nanopowder sample (99%), 2,2′-(ethylenedioxy)bis(ethylamine) (EDA), and poly(vinyl alcohol) (PVA, M_W ~ 90,000) were purchased from Sigma-Aldrich, thionyl chloride (>99%) from Alfa Aesar, nitric acid from VWR, and sulfuric acid (98%) from Fisher Scientific. Dialysis membrane tubing (cutoff molecular weight ~ 500) was supplied by Spectrum Laboratories. Water was deionized and purified by being passed through a LabconcoWaterPros water purification system.

Measurement

Eppendorf centrifuge (model 5417 R) was used for centrifugation at various *g* values. Transmission electron microscopy (TEM) images were obtained on a Hitachi H-7600 instrument operated at 100–120 kV. Atomic force microscopy (AFM) analysis was carried out in the acoustic AC mode on a Molecular Imaging PicoPlus AFM system equipped with a multipurpose scanner and a NanoWorldPointprobe NCH sensor. The height profile analysis was assisted by using the SjPIP software distributed by Image Metrology.

Optical absorption spectra were recorded on a Shimadzu UV2501-PC spectrophotometer. Fluorescence spectra were measured on a Jobin-Yvon emission spectrometer equipped with a 450 W xenon source, Gemini-180 excitation and Tirax-550 emission monochromators, and a photon-counting detector (Hamamatsu R928P PMT at 950 V). Fluorescence decays were measured on a time-correlated single photon counting (TCSPC) setup with a Hamamatsu stabilized picosecond light pulser (PLP-02) for 407 nm excitation (<100 ps pulses at 1 MHz repetition rate), coupled with a Phillips XP2254/B PMT in a thermoelectrically cooled housing as a detector for an overall instrument time resolution of 500 ps or better.

A specifically designed film sample holder for being used in the emission spectrometer was made by using 3D printing in house (see also Supplementary Information). The physical dimensions of the holder march exactly those of a standard 1 cm cuvette, so that the holder is fully compatible with the sample chamber in the emission spectrometer. The outer piece

of the holder is equivalent to a typical plastic cuvette, except for large openings at all four sides. Inside the outer piece is fitted precisely in the diagonal geometry a pair of composite plates, both of which have a matching large opening in the center. The function of the plates is to sandwich a film specimen for fluorescence measurements in such a geometry that the film is excited in the back with a 45° angle to the excitation light, and the emissions are collected in the front of the film also in a 45° angle to the detector. The performance of the sample holder in terms of reproducibility and reliability in the measurement of film samples against fluorescence film standard (rhodamine 6G in PVA film) was evaluated by repeated measurements of sample and/or standard films, and in each measurement the selected film was reloaded into the holder. The variations in measurement results were around 5% or less, which were considered as being sufficient for the validation of the sample holder.

Carbon Nanoparticles and EDA-Carbon Dots

The commercially acquired carbon nanopowder sample was refluxed in aqueous nitric acid (2.6 M) for 24 h, washed with deionized water repeatedly, and then dried under nitrogen. The treated sample (200 mg) was further treated in the mixed acid of concentrated sulfuric acid and nitric acid (3/1 v/v, 10 mL) at 60 °C with sonication for 1 h and then refluxing for 2 h. To the resulting mixture was added deionized water (100 mL) for centrifugation at 20,000 *g* for 30 min to keep the supernatant. It was dialyzed in a membrane tubing (cutoff molecular weight ~ 500) against fresh water for 3 days to yield a stable dispersion of carbon nanoparticles.

For the synthesis of EDA-carbon dots, the nitric acid treated carbon nanopowder sample discussed above was dialyzed in a membrane tubing (cutoff molecular weight ~ 500) against fresh water, followed by centrifugation at 1,000 *g* to retain the supernatant as a suspension of carbon nanoparticles. The nanoparticles were recovered by the removal of water via evaporation, and then refluxed in neat thionyl chloride for 12 h. Upon the removal of excess thionyl chloride, the treated sample (50 mg) was mixed well with carefully dried (vacuum oven at ~60 °C for 4 h) EDA liquid in a round-bottom flask, heated to 120 °C, and vigorously stirred under nitrogen protection for 3 days. The reaction mixture back at room temperature was dispersed in water and then centrifuged at 20,000 *g* to retain the supernatant. It was dialyzed in a membrane tubing (cutoff molecular weight ~ 500) against fresh water to remove unreacted EDA and other small molecular species to obtain an aqueous solution of the as-synthesized EDA-carbon dots. A Sephadex™ G-100 gel column (packed in house with commercially supplied gel sample) was used for the fractionation of the as-synthesized sample by following the experimental protocol already reported in the literature.[24]

PVA Films

PVA polymer (M_W ~ 90,000, 750 mg) was dissolved in deionized water (10 mL) at 80 °C. Separately, aqueous solution with known concentration of a selected sample of EDA-carbon dots was prepared, and a quantitatively measured amount of the solution was mixed with the PVA solution under vigorous stirring. The resulting solution was degassed, concentrated by the evaporation of water until viscous, and then drop-casted onto a clean glass slide. The film thickness was controlled by controlling the amount of material used for casting and the

film dimensions on the slide. After drying, the PVA/carbon dots composite film was peeled off the slide to be free-standing. The same procedure was applied to the fabrication of PVA films embedded with carbon nanoparticles or rhodamine 6G as fluorescence standard.

Results and Discussion

Carbon nanoparticles were harvested from commercially supplied carbon nanopowder sample in procedures including the sample being subjected to several acid treatment steps involving aqueous nitric acid and the mixed acid composed of concentrated sulfuric acid and nitric acid.[18] The acid treated sample was dialyzed against fresh water, and centrifuged to keep the supernatant as an aqueous dispersion of carbon nanoparticles, which appeared transparent and solution-like (Figure 2). The treatment with the mixed acid was apparently a necessary step in the processing to make the resulting dispersion relatively more stable without any meaningful precipitation. The dispersed carbon nanoparticles were small, as desired, on average around 4.5 nm according to results from the transmission electron microscopy (TEM) characterization (Figure 3). The broad optical absorption spectrum of the aqueous dispersed carbon nanoparticles is also shown in Figure 2.

The carbon nanoparticles in aqueous dispersion were found to be weakly fluorescent (Figure 2), with observed quantum yields on the order of 1–2%, and somewhat different at different excitation wavelengths. The results are in general agreement with those already reported in the literature.[19–23] It has been argued that even without the deliberate surface passivation via the kind of organic functionalization in carbon dots, the solvation of the carbon nanoparticles in an aqueous medium may provide some passivation effect to result in the observed relatively weak fluorescence emissions.[6,21]

The carbon nanoparticles were functionalized with 2,2′-(ethylenedioxy)bis(ethylamine) (EDA) under amidation reaction conditions to obtain EDA-carbon dots, as reported previously.[33] The as-synthesized sample was readily soluble in water, thus cleaned in dialysis (through membrane tubing with cutoff molecular weight ~ 500) to remove unreacted EDA and other small molecular species. Results from atomic force microscopy (AFM) characterization (Figure 4) suggested that the carbon dots were on the order of 5 nm in diameter, consistent with the TEM results on the sizes of precursor carbon nanoparticles (Figure 3).

Absorption and fluorescence spectra of the as-synthesized sample of EDA-carbon dots in aqueous solution are shown in Figure 5. The observed fluorescence quantum yields were much higher than those of the aqueous dispersed carbon nanoparticles, 15–20% (varying from batch to batch in duplicating syntheses) at 400 nm excitation. Since the as-synthesized sample was generally known as a mixture of EDA-carbon dots of different fluorescence quantum yields,[33] an aqueous gel column (Sephadex™G-100) was used for the fractionation of the sample,[24] yielding fractions of fluorescence quantum yields higher or lower than the pre-fractionation average (Figure 5). As discussed in the literature, the difference in fluorescence brightness between different fractions reflects upon the effectiveness of surface passivation in the corresponding carbon dots.[24,34] Therefore, fractions of the carbon dots exhibiting lower fluorescence quantum yields due to relatively less effective surface

passivation should be expected to benefit more significantly from any external effect that would improve the surface passivation, such as the expected compression effect experienced by the carbon dots embedded in a polymer film matrix. This was confirmed in the film study in which a fraction combining the EDA-carbon dots of fluorescence quantum yields around 5% at 400 nm excitation was used as the starting point.

Poly(vinyl alcohol) (PVA) was selected as the polymer host for its known high optical quality and desirable film properties.[35–37] In the fabrication of polymeric nanocomposite films with embedded EDA-carbon dots, the selected sample solution was added dropwise to a separately prepared aqueous solution of PVA with stirring to obtain a homogeneous mixture. The mixture was degassed thoroughly (centrifuged vigorously and then sonicated in the degas mode), concentrated until viscous, and drop-casted onto a clean glass slide. Upon drying, the PVA/EDA-carbon dots film was peeled off the slide to be free-standing (Figure 6). Blank PVA film without carbon dots was prepared in the same procedure. The film thickness was controlled in the fabrication by using the same amount of PVA and by keeping the film dimensions as constant as possible.

The PVA/carbon dots composite films appeared colored, but optically transparent (Figure 6). The observed absorption spectra of the EDA-carbon dots in PVA film (as blank film has no absorption in the same spectral region) are largely the same as those in solution (Figures 5 & 6). Since the optical absorption of carbon dots is due to transitions associated with the π-plasmon in the core carbon nanoparticles, the results suggest that the film environment has no significant effect on the transitions. The observed fluorescence spectra of the EDA-carbon dots in PVA film are also similar to those in solution at same excitation wavelengths, except for slight blue shifts due to the film environment (Figure 6). The composite films were visually brightly fluorescent under light illumination, suggesting substantial fluorescence quantum yields.

Fluorescence quantum yields of the EDA-carbon dots in PVA films were determined quantitatively by using the relative method with a film of rhodamine 6G in PVA as fluorescence standard, for which the assumed no effect on the fluorescence quantum yield of the dye by PVA was justified by the experimental results such that in a comparison of rhodamine 6G in aqueous solutions without and with high concentrations of PVA (up to 200 mg/mL, with the solution becoming viscous to mimic conditions in films), no meaningful changes in fluorescence intensities were observed. However, because of the implicit assumptions behind the relative method,[38] an absolute requirement is for the sample and the standard to have the same configuration (film vs film) and also the same measurement geometry in the fluorescence spectrometer.[38,39] The latter is intrinsically more difficult for film specimens, requiring special effort in terms of instrumental setup and measurements. Therefore, a film sample holder was specifically designed and constructed (details in Experimental Section) for the fluorescence spectrometer to ensure the same measurement geometry for the films and thus the reproducibility in the measurement of their fluorescence intensities. As a calibration to evaluate and demonstrate the reproducibility, several PVA/rhodamine 6G films were used for multiple independent (film remounted in the holder each time) measurements, equivalent to multiple independent determinations of the fluorescence quantum yield of a PVA/rhodamine 6G film by using itself or another film of the same kind

as fluorescence standard. The results suggested that the variation over multiple films, each with multiple independent measurements, was around 5%, an error margin not so different from that in the use of the relative method for fluorescence quantum yield determination in general. Therefore, the same film sample holder and measurement protocol were used in the determination of fluorescence quantum yields of all PVA/carbon dots films in reference to the PVA/rhodamine 6G film standard. For the same sample film over multiple independent measurements, the variation in the resulting fluorescence quantum yield values was also on the order of 5%. As shown in Figure 7, the fraction of EDA-carbon dots with the solution-phase fluorescence quantum yield of 5% (400 nm excitation) exhibited nearly a doubling in the yield upon being incorporated into the PVA film matrix (Figure 7).

The enhancement in fluorescence quantum yields from solution to film was apparently more dramatic relatively (in terms of the percentage increase) for less fluorescent fractions of the EDA-carbon dots. For example, the fraction from the gel column separation with a fluorescence quantum yield of around 15% in aqueous solution (400 nm excitation) was used in the fabrication of PVA/carbon dots composite films, and the fluorescence quantum yields in films were also determined in reference to the PVA/rhodamine 6G film standard by using the same film sample holder and measurement protocol. The enhancement from solution to film was significant, with the observed fluorescence quantum yield increased to more than 20% in film, though seemingly less dramatic in the percentage term (a 50% increase from solution to film, Figure 7). Similar enhancement from solutions to films was confirmed with films fabricated by using other fractions of the EDA-carbon dots of different solution-phase fluorescence quantum yields, as also illustrated in Figure 7. In control experiments, fluorescence quantum yields of EDA-carbon dots in aqueous solutions were measured in the presence of PVA in various concentrations (up to 200 mg/mL), no meaningful changes were observed.

For carbon dots of the same surface functional molecules, the gel-column separated fractions of different observed fluorescence quantum yields have generally been correlated with different levels of surface functionalization-passivation in the corresponding carbon dots, those less well functionalized-passivated exhibiting lower fluorescence quantum yields.[24,34] In this regard, at the limit is the aqueous dispersed carbon nanoparticles without surface functionalization (depending on solvation for relatively weak surface passivation effect).[23] Therefore, the particle dispersion was also used for the fabrication of PVA/carbon nanoparticles composite films, and their fluorescence quantum yields were similarly determined. The results suggested the most significant percentage increases in fluorescence quantum yields from the aqueous dispersion to composite films (Figure 7).

Within the mechanistic framework discussed in the introduction section, the observed substantial increases in fluorescence quantum yields of carbon dots from solutions to PVA films are attributed primarily to significantly enhanced surface passivation effect on the carbon nanoparticles in carbon dots in the film environment. Similar observations in the literature on solid-state matrix effect on the embedded carbon dots may be understood in terms of the same mechanistic origins.[30,40] In the PVA/carbon dots composite films, while PVA may not add directly to the surface passivation layer in carbon dots (Figure 1), the film environment may compress the existing EDA functionalization to enhance the surface

passivation effect to result in brighter fluorescence emissions across all fractions of the EDA-carbon dots with different solution-phase fluorescence quantum yields (Figure 7). Similarly, it may be argued that such a film environment-induced effect is more significant relatively on the less fluorescent factions. At the extreme for “naked” carbon nanoparticles in PVA film matrix, the matrix polymers are apparently able to provide more effective surface passivation than water molecules in aqueous dispersion of the nanoparticles for largest percentage increase in the observed fluorescence quantum yield. Nevertheless, in absolute terms the incorporation of the most fluorescent fraction of EDA-carbon dots into PVA films resulted in the substantial improvement to push the fluorescence quantum yield over 40% (Figure 7).

The film environment-induced fluorescence quantum yield enhancement (or “negative quenching effect” in a different description)[23] must be mostly static in nature, generally manifested in terms of a decoupling between fluorescence intensity quenching and fluorescence lifetime quenching.[38] This was confirmed by the results from fluorescence decay measurements based on the time-correlated single photon counting (TCSPC). As compared in Figure 8, the decay curve of the EDA-carbon dots in PVA film is essentially the same as that in solution, despite the substantially higher fluorescence quantum yield observed in the same film sample. Both decay curves could not be deconvoluted with a mono- or bi-exponential function, suggesting a distribution of fluorescence lifetimes.

In addition to the results shown in Figure 7 for 400 nm excitation, enhanced fluorescence quantum yields in representative sample films at other excitation wavelengths were determined and compared. Shown in Figure 9 are results for the films corresponding to the fractions of EDA-carbon dots with solution-phase fluorescence quantum yields of around 5%, 15%, and 32% at 400 nm excitation. Across all of the excitation wavelengths, there are significant increases in the observed fluorescence quantum yields from solution to films, with the film-to-solution ($\Phi_{F,film}/\Phi_{F,solution}$) ratio varying with the excitation wavelength (Figure 9). The variation is such that the enhancements at longer excitation wavelengths are more pronounced than at 400 nm excitation. For the more fluorescent film (Figure 9), the $\Phi_{F,film}/\Phi_{F,solution}$ ratios at 480 nm and 520 nm excitations are 2.3 and 1.9, corresponding to absolute fluorescence quantum yield values in the film of 10% and 4%, respectively. The results suggest that the incorporation of carbon dots into polymer films or other optically transparent matrices may be further explored as a strategy for the general need to increase the fluorescence brightness of carbon dots at longer excitation wavelengths.

In addition to mechanistic implications of the results presented above on enhanced surface passivation effect with carbon dots embedded in a more confined environment in polymer matrix, technologically an improved understanding of polymeric composites with brightly fluorescent carbon dots is relevant to the increasing interest in using carbon dots for optoelectronic devices, light emitting diodes (LEDs) in particular.[41,42] A potentially more direct use of the polymer/carbon dots composite films is to take advantage of their bright fluorescence emissions for displays, signs, or other luminescence-based devices.

Conclusions

Carbon dots are small carbon nanoparticles with various surface passivation schemes, among which the most effective has been the particle surface functionalization. As a result, the fluorescence properties of carbon dots, the brightness or quantum yields in particular, are sensitive to the level and effectiveness of the surface functionalization-passivation, as reflected by the different performances of the fractions from separating the as-synthesized sample of EDA-carbon dots. Demonstrated in this work is that in all fractions the passivation effect could be enhanced significantly upon dispersing the carbon dots into a polymer (PVA) film matrix, corresponding to observed higher fluorescence quantum yields. The fluorescence decay results suggest that the enhanced passivation effect is static in nature. Mechanistically the enhancement may be rationalized as being associated with the compression of the surface passivation layer (similar to a soft corona) in carbon dots embedded in the more restrictive film environment, which must have provided stabilization effect on the trapped electrons and holes for more efficient radiative recombinations. Technologically, the brightly fluorescent polymer/carbon dots composite films with multiple emission colors may find direct or indirect applications in various optical or optoelectronic devices, from fluorescent displays to LEDs.

Supplementary Material

Refer to Web version on PubMed Central for supplementary material.

Acknowledgments

Financial support from NSF and NIH (Y.-P.S.), the Air Force Office of Scientific Research through Dr. Michael Berman (C.E.B.), and the Air Force Research Laboratory (C.E.B.) is gratefully acknowledged. H.M. was on leave from Xinjiang University in Urumqi, China and Z.-L.H. on leave from Beijing University of Chemical Technology in Beijing, China, both with visiting scholarships provided by the China Scholarship Council.

Notes and references

1. Sun Y-P, Zhou B, Lin Y, Wang W, Fernando KAS, Pathak P, Meziani MJ, Harruff BA, Wang X, Wang HF, Luo PJG, Yang H, Kose ME, Chen BL, Veca LM, Xie SY. J Am Chem Soc. 2006; 128:7756–7757. [PubMed: 16771487]
2. Cao L, Wang X, Meziani MJ, Lu F, Wang H, Luo PG, Lin Y, Harruff BA, Veca LM, Murray D, Xie SY, Sun Y-P. J Am Chem Soc. 2007; 129:11318–11319. [PubMed: 17722926]
3. Luo PG, Sahu S, Yang ST, Sonkar SK, Wang J, Wang H, LeCroy GE, Cao L, Sun YP. J Mat Chem B. 2013; 1:2116–2127.
4. Luo PG, Sonkar SK, Yang ST, Yang F, Yang L, Broglie JJ, Sun YP. RSC Adv. 2014; 4:10791–10807.
5. Miao P, Han K, Tang Y, Wang B, Lin T, Cheng W. Nanoscale. 2015; 7:1586–1595. [PubMed: 25510876]
6. Cao L, Meziani MJ, Sahu S, Sun Y-P. Acc Chem Res. 2013; 46:171–180. [PubMed: 23092181]
7. Wang Y, Hu A. J Mater Chem C. 2014; 2:6921–6939.
8. Hola K, Zhang Y, Wang Y, Giannelis EP, Zboril R, Rogach AL. Nano Today. 2014; 9:590–603.
9. Lim SY, Shen W, Gao Z. Chem Soc Rev. 2015; 44:362–381. [PubMed: 25316556]
10. Zhao A, Chen Z, Zhao C, Gao N, Ren J, Qu X. Carbon. 2015; 85:309–327.
11. Wang J, Qiu J. J Mater Sci. 2016; 51:4728–4738.

12. Fernando KAS, Sahu S, Liu Y, Lewis WK, Guliants EA, Jafariyan A, Wang P, Bunker CE, Sun Y-P. ACS Appl Mater Interfaces. 2015; 7:8363–8376. [PubMed: 25845394]
13. Du Y, Guo S. Nanoscale. 2016; 8:2532–2543. [PubMed: 26757977]
14. Konstantinos D. Curr Org Chem. 2016; 20:682–695.
15. Hu C, Yu C, Li M, Wang X, Yang J, Zhao Z, Eychmüller A, Sun YP, Qiu J. Small. 2014; 10:4926–4933. [PubMed: 25048718]
16. Hu C, Yu C, Li M, Wang X, Dong Q, Wang G, Qiu J. Chem Commun. 2015; 51:3419–3422.
17. Wu M, Wang Y, Wu W, Hu C, Wang X, Zheng J, Li Z, Jiang B, Qiu J. Carbon. 2014; 78:480–489.
18. Li M, Hu C, Yu C, Wang S, Zhang P, Qiu J. Carbon. 2015; 91:291–297.
19. Ray SC, Saha A, Jana NR, Sarkar R. J Phys Chem C. 2009; 113:18546–18551.
20. Lu J, Yang J-x, Wang J, Lim A, Wang S, Loh KP. ACS Nano. 2009; 3:2367–2375. [PubMed: 19702326]
21. Ciftan Hens S, Lawrence WG, Kumbhar AS, Shenderova O. J Phys Chem C. 2012; 116:20015–20022.
22. Liu J-H, Yang S-T, Wang X, Wang H, Liu Y, Luo PG, Liu Y, Sun Y-P. ACS Appl Mater Interfaces. 2014; 6:14672–14678. [PubMed: 25068474]
23. Cao L, Anilkumar P, Wang X, Liu J-H, Sahu S, Meziani MJ, Myers E, Sun Y-P. Can J Chem. 2011; 89:104–109.
24. Wang X, Cao L, Yang S-T, Lu F, Meziani MJ, Tian L, Sun KW, Bloodgood MA, Sun Y-P. Angew Chem Int Ed. 2010; 49:5310–5314.
25. Dong Y, Wang R, Li H, Shao J, Chi Y, Lin X, Chen G. Carbon. 2012; 50:2810–2815.
26. Li X, Zhang S, Kulinich SA, Liu Y, Zeng H. Sci Rep. 2014; 4:4976–4984.
27. Bao L, Liu C, Zhang Z-L, Pang D-W. Adv Mater. 2015; 27:1663–1667. [PubMed: 25589141]
28. Chandra S, Pathan SH, Mitra S, Modha BH, Pramanik P, Goswami A. RSC Advances. 2012; 2:3602–3606.
29. Cao L, Sahu S, Anilkumar P, Bunker CE, Xu J, Fernando KAS, Wang P, Guliants EA, Tackett KN, Sun YP. J Am Chem Soc. 2011; 133:4754–4757. [PubMed: 21401091]
30. Xie Z, Wang F, Liu C-y. Adv Mater. 2012; 24:1716–1721. [PubMed: 22396335]
31. Zhou L, He B, Huang J. Chem Commun. 2013; 49:8078–8080.
32. Hao Y, Gan Z, Xu J, Wu X, Chu PK. Appl Surf Sci. 2014; 311:490–497.
33. LeCroy GE, Sonkar SK, Yang F, Veca LM, Wang P, Tackett KN, Yu JJ, Vasile E, Qian H, Liu Y, Luo P, Sun YP. ACS Nano. 2014; 8:4522–4529. [PubMed: 24702526]
34. Anilkumar P, Wang X, Cao L, Sahu S, Liu J-H, Wang P, Korch K, Tackett Ii KN, Parenzan A, Sun Y-P. Nanoscale. 2011; 3:2023–2027. [PubMed: 21350751]
35. Michl, J., Bonacic-Koutechy, V. Electronic Aspects of Organic Photochemistry. John Wiley & Sons; New York: 1990.
36. Zhou B, Lin Y, Veca LM, Fernando KAS, Harruff BA, Sun YP. J Phys Chem B. 2006; 110:3001–3006. [PubMed: 16494301]
37. Hourd AC, Baker RT, Abdolvand A. Nanoscale. 2015; 7:13537–13546. [PubMed: 26204243]
38. Lakowicz, RJ. Principles of Fluorescence Spectroscopy. 2nd. Kluwer Academic/Plenum Publisher; New York: 1999.
39. Würth C, Grabolle M, Pauli J, Spieles M, Resch-Genger U. Nat Protocols. 2013; 8:1535–1550. [PubMed: 23868072]
40. Müller M, Kaiser M, Stachowski GM, Resch-Genger U, Gaponik N, Eychmüller A. Chem Mat. 2014; 26:3231–3237.
41. Mao L-H, Tang W-Q, Deng Z-Y, Liu S-S, Wang C-F, Chen S. Ind Eng Chem Res. 2014; 53:6417–6425.
42. Sarswat PK, Free ML. Phys Chem Chem Phys. 2015; 17:27642–27652. [PubMed: 26426733]

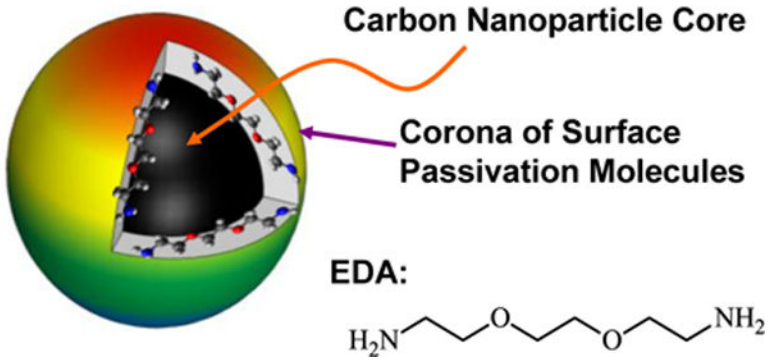

Figure 1.

A cartoon illustration on EDA-carbon dot, generally a small carbon nanoparticle core with attached and strongly adsorbed EDA molecules for surface passivation (a configuration similar to a soft corona).

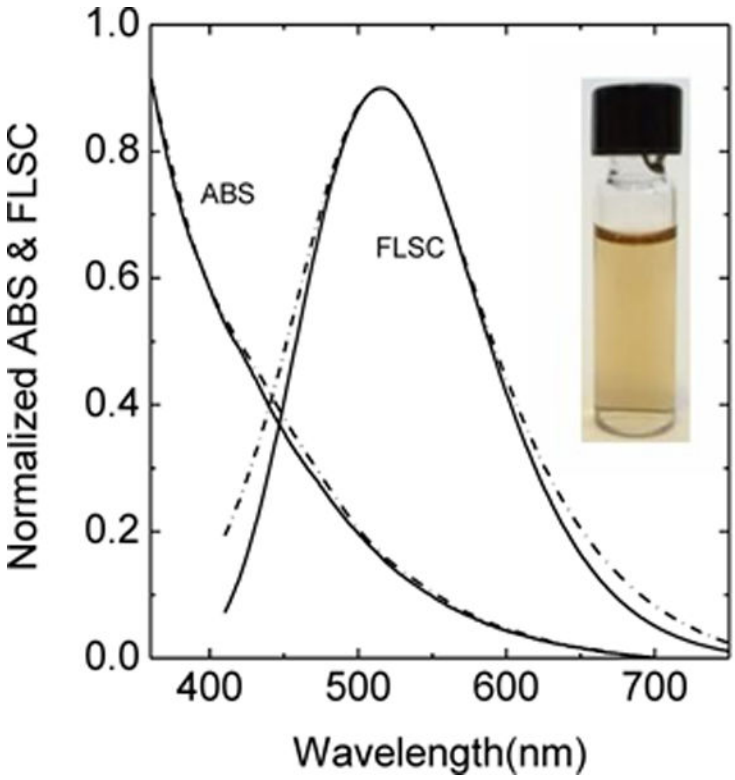

Figure 2.

Absorption (ABS) and fluorescence (FLSC, 400 nm excitation) spectra of carbon nanoparticles in aqueous dispersion (—, with a photograph on the dispersion in the inset) and in PVA film (– · – · –).

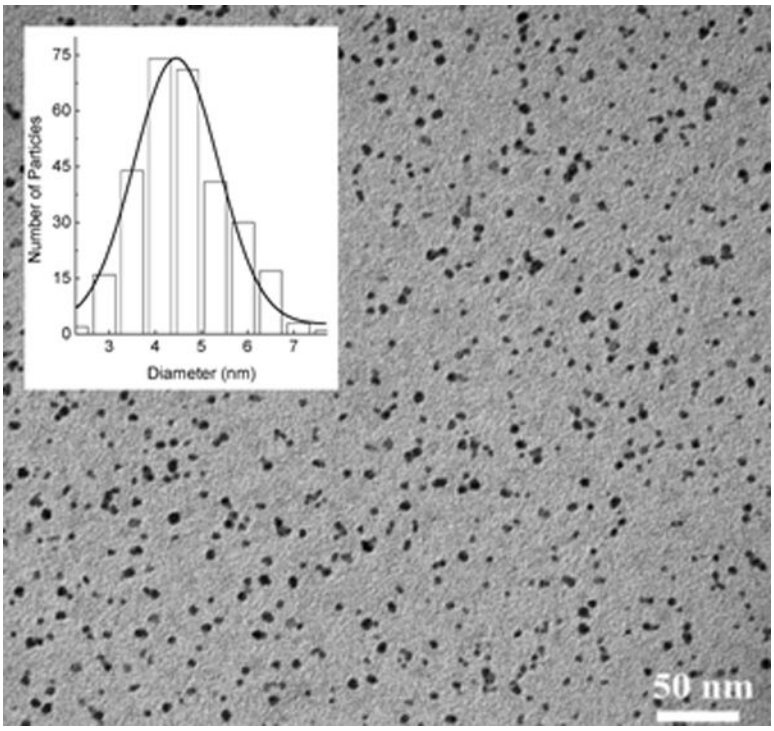

Figure 3.

A representative TEM image of the carbon nanoparticles, with the size distribution analysis in the inset.

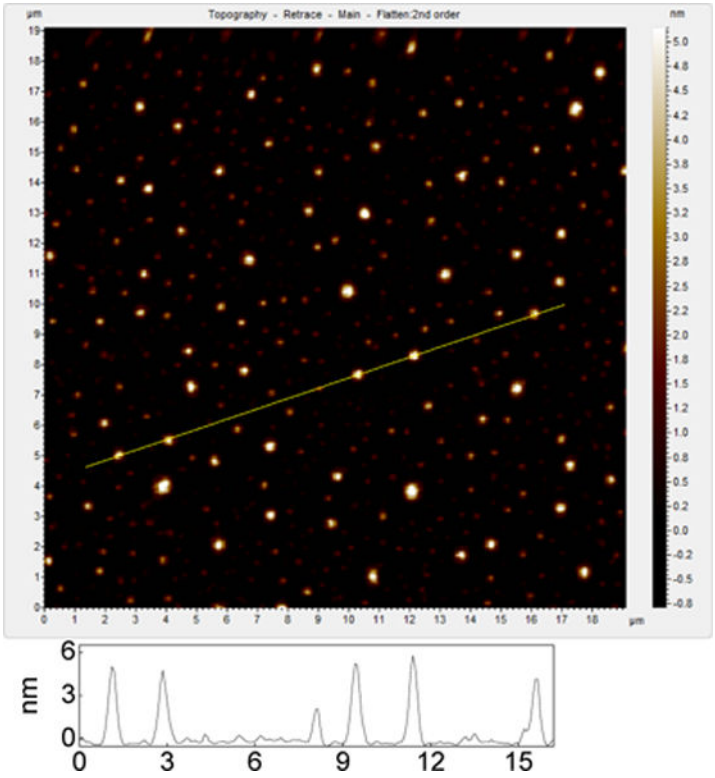

Figure 4.
Results from AFM imaging of the EDA-carbon dots on mica, with height analyses on selected dots for estimating their sizes.

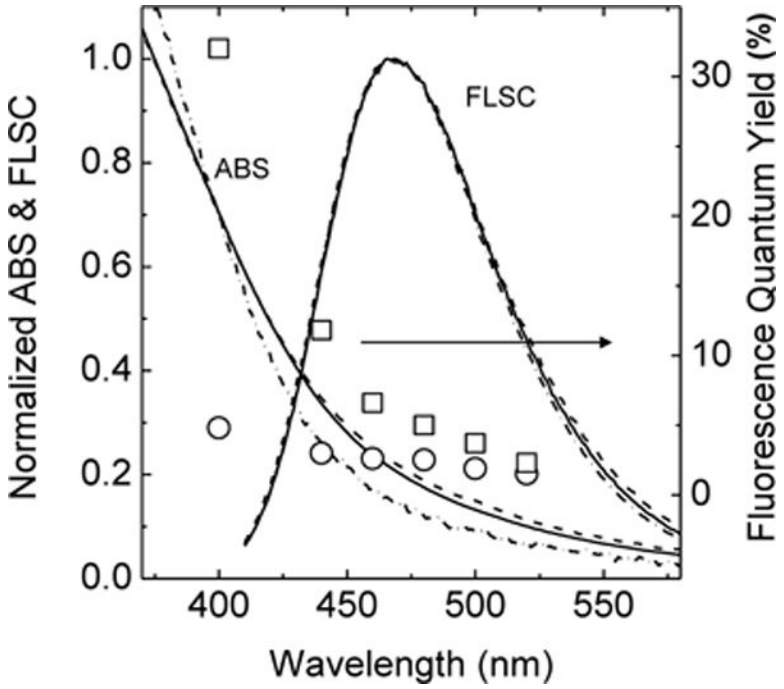

Figure 5.

Absorption (ABS) and fluorescence (FLSC, 400 nm excitation) spectra of the EDA-carbon dots in aqueous solution (the as-prepared sample: —; the separated fractions with fluorescence quantum yields at 400 nm excitation of around 5%: – – – and 32%: – · – · –), and observed fluorescence quantum yields of the two fractions at different excitation wavelengths (the lower-yield fraction: circles, and the higher-yield fraction: squares).

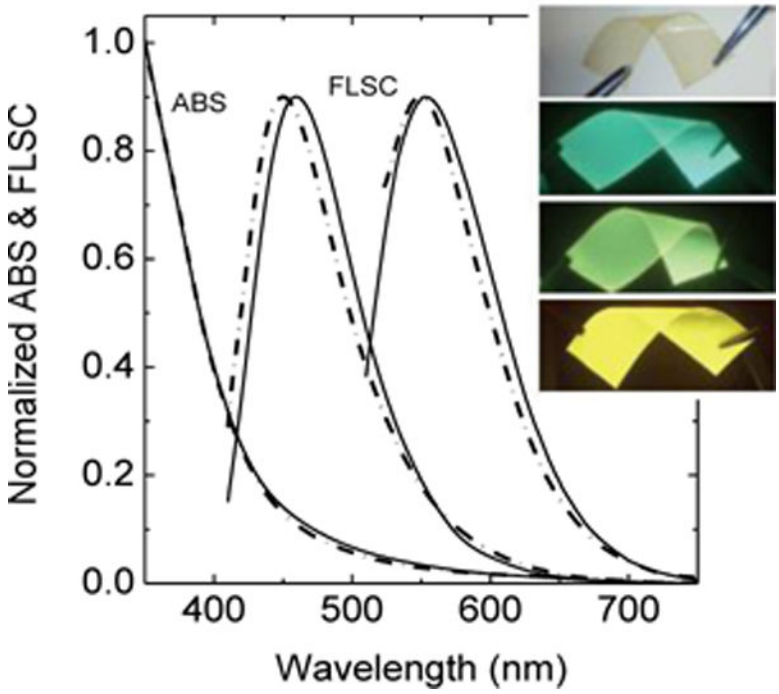

Figure 6.

Absorption (ABS) and fluorescence (FLSC, 400 nm excitation on the left and 500 nm excitation on the right) spectra of the EDA-carbon dots in aqueous solution (—) and in PVA film (– · – · –). Inset: Photographs on the PVA/carbon dots composite film (from top to bottom) under ambient light and exposed to a UV lamp (350–400 nm, with the three photos taken through 405 nm, 475 nm, and 525 nm cutoff filters).

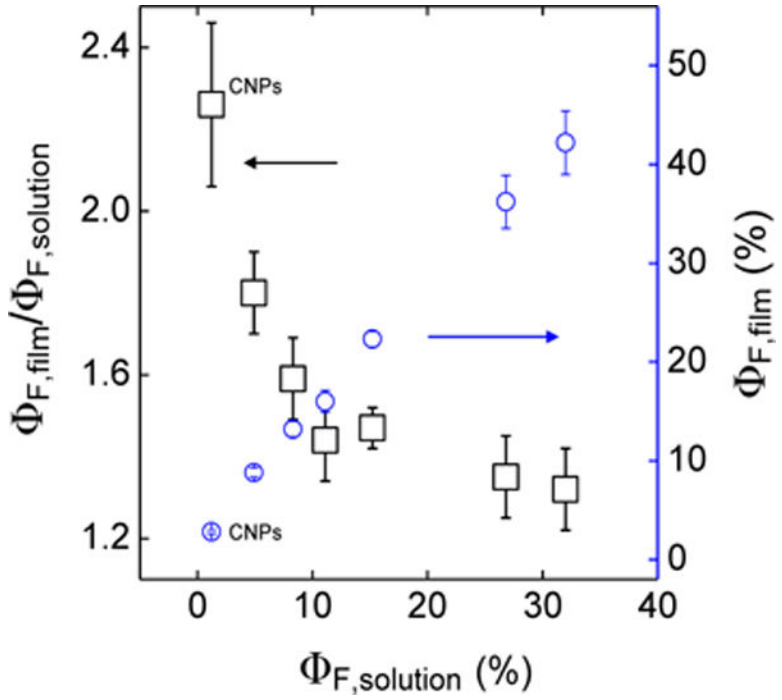

Figure 7.

Fluorescence quantum yields of the separated fractions of the EDA-carbon dots (including naked carbon nanoparticles or CNPs) in PVA films ($\Phi_{F,film}$) vs in solution ($\Phi_{F,solution}$): circles; and a plot of the enhancement factor $\Phi_{F,film}/\Phi_{F,solution}$ vs $\Phi_{F,solution}$: squares.

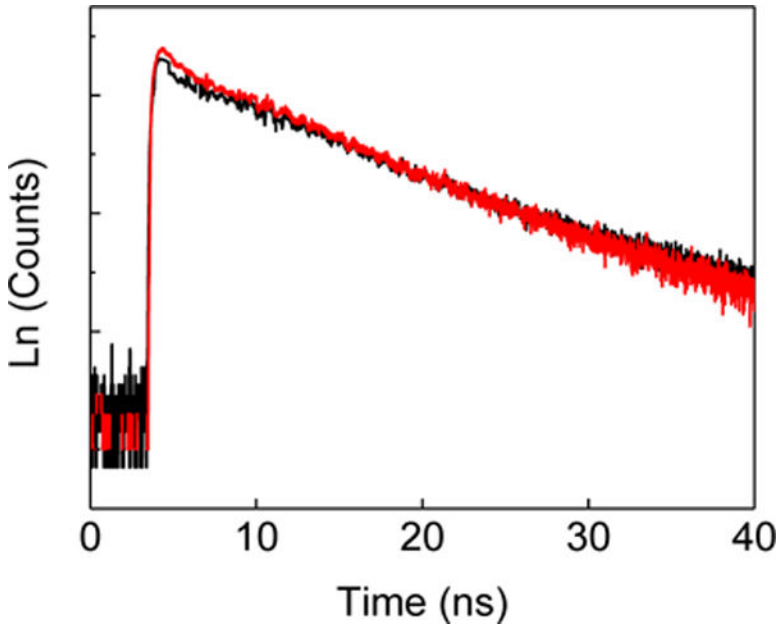

Figure 8.

A comparison between fluorescence decay curves of the EDA-carbon dots in aqueous solution (black) and in PVA film (red).

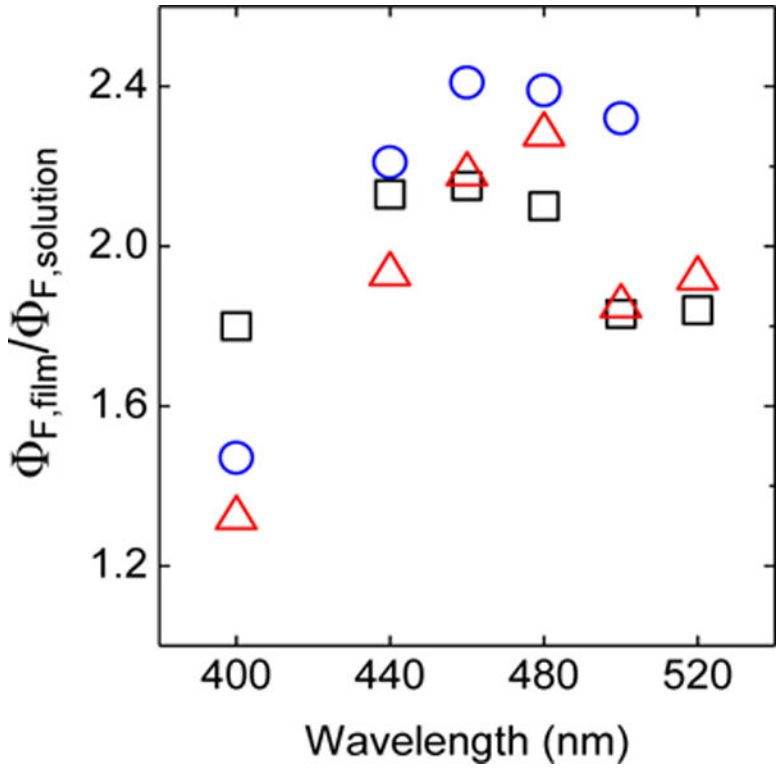

Figure 9.

Excitation wavelength dependencies of the fluorescence quantum yield enhancements from aqueous solution to PVA film (as measured by $\Phi_{F,film}/\Phi_{F,solution}$) for different EDA-carbon dots fractions with solution-phase quantum yields at 400 nm excitation of around 5% (squares), 15% (circles), and 32% (triangles).